Odd-harmonic Repetitive Control of an Active Filter under Varying Network Frequency: Control Design and Stability Analysis

Josep M. Olm, Germán A. Ramos, Ramon Costa-Castelló, Rafael Cardoner

Abstract— This work deals with the design and analysis of a controller for a shunt active power filter. The design is based on combined feedforward and feedback actions, the last using repetitive control, and aims at the obtention of a good closed-loop performance in spite of the possible frequency variations that may occur in the electrical network. As these changes affect the performance of the controller, the proposal includes a compensation technique consisting of an adaptive change of the digital controller's sampling time according to the network frequency variation. However, this implies structural changes in the closed-loop system that may destabilize the overall system. Hence, this article is also concerned with closed-loop stability of the resulting system, which is analyzed using a robust control approach through the small gain theorem. Experimental results that indicate good performance of the closed-loop system are provided.

I. INTRODUCTION

The control of shunt active filters can be carried out using different approaches [1], [2]. Most of them are based on two hierarchical control loops, an inner one in charge of assuring the desired current and an outer one in charge of determining the required shape as well as the appropriate power balance.

In this work, the current controller is composed of a feed-forward action that provides very fast transient response and an odd-harmonic repetitive control law yielding closed-loop stability and a very good harmonic correction performance [3]. The outer control law is based on the exact computation of the sinusoidal current network amplitude and, in order to improve robustness, this computation is combined with a feedback control law including an analytically tuned PI controller [3]. This control algorithm depends on network voltage frequency and shows a dramatic performance decay when this value is not properly know or changes in time. This article proposes an adaptation of the controller sampling rate according to the disturbance/reference period [4], [5], [6], [7].

In this paper, both the inner and the outer loop adapt their sampling frequency to the period of the signal being tracked. This allows to preserve the steady-state performance while maintaining a low computational cost. Nevertheless,

R. Costa-Castelló and R. Cardoner are with the Institute of Industrial and Control Engineering, Universitat Politècnica de Catalunya, Av. Diagonal, 647 08028 Barcelona, Spain `ramon.costa@upc.edu`, `rafael.cardoner@upc.edu`

J. M. Olm, corresponding author, is with the Department of Applied Mathematics IV, Universitat Politècnica de Catalunya, Avda. Víctor Balaguer, s/n, 08800 Vilanova i la Geltrú, Spain `josep.olm@upc.edu`

G.A. Ramos is with the Department of Electrical and Electronic Engineering, Universidad Nacional de Colombia, Bogotá DC, Colombia e-mail: `garamosf@unal.edu.co`

the structural changes induced by this operation, which transforms an original Linear Time Invariant system (LTI) into a Linear Time-Varying (LTV) one, may destabilize the closed-loop system. Hence, we use the small-gain theorem-based technique introduced in [8] to find out stability margins where reliable performance is definitely ensured.

This adaptive procedure, along with the introduction of feedforward paths, yield very good performance both in transient and in steady-state behavior, as well as robustness in front of network frequency variations for which stability margins are derived.

II. STATEMENT OF THE PROBLEM

A. The boost converter

The system architecture is depicted in Fig. 1. A load is connected to the power source, while an active filter is applied in parallel in order to fulfill the desired behavior, i.e. to guarantee unity power factor at the network side. A boost converter with the ac neutral wire connected directly to the midpoint of the dc bus is used as active filter. The averaged (at the switching frequency) model of the boost converter is given by

$$L\frac{di_f}{dt} = -r_L i_f - v_1 \frac{d+1}{2} - v_2 \frac{d-1}{2} + v_n \quad (1)$$

$$C_1 \frac{dv_1}{dt} = -\frac{v_1}{r_{C,1}} + i_f \frac{d+1}{2} \quad (2)$$

$$C_2 \frac{dv_2}{dt} = -\frac{v_2}{r_{C,2}} + i_f \frac{d-1}{2} \quad (3)$$

where d is the duty ratio, i_f is the inductor current and v_1, v_2 are the dc capacitor voltages; $v_n = V_n \sqrt{2} \sin(\omega_n t)$ is the voltage source,[1] L is the converter inductor, r_L is the inductor parasitic resistance, C_1, C_2 are the converter capacitors and $r_{C,1}$, $r_{C,2}$ are the parasitic resistances of the capacitors. The control variable, d, takes its value in the closed real interval $[-1, 1]$ and represents the averaged value of the Pulse-Width Modulation (PWM) control signal injected to the actual system.

Due to the nature of the voltage source, the steady-state load current is usually a periodic signal with only odd-harmonics in its Fourier series expansion, so it can be written as $i_l = \sum_{k=0}^{\infty} a_k \sin(\omega_n(2k+1)t) + b_k \cos(\omega_n(2k+1)t)$.

B. Control objectives

The active filter goal is to assure that the load is seen as a resistive one. This can be stated as $i_n^* = I_d^* \sin(\omega_n t)$, i.e. the

---

[1] $\omega_n = 2\pi/T_p$ rad/s is the network frequency.
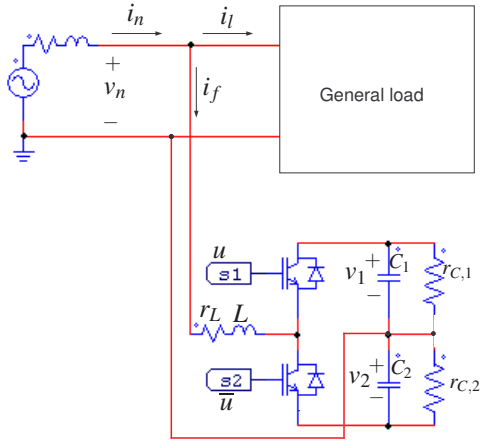
Fig. 1. Single-phase shunt active filter connected to the network-load system.

source current must have a sinusoidal shape in phase with the network voltage[2]. Another collateral goal, necessary for a correct operation of the converter, is to assure constant average value of the dc bus voltage[3], i.e. $<v_1 + v_2 >_0^* = v_d$, where v_d must fulfill the boost condition ($v_d > 2\sqrt{2}v_n$). It is also desirable for this voltage to be almost equally distributed among both capacitors ($v_1 \approx v_2$).

C. Transforming the plant equations

It is standard for this type of systems to linearize the current dynamics by the partial state feedback $\alpha = \frac{d+1}{2}v_1 + \frac{d-1}{2}v_2$. Moreover, the change of variables

$$i_f = i_f, \quad E_C = \frac{1}{2}\left(C_1 v_1^2 + C_2 v_2^2\right), \quad D = C_1 v_1 - C_2 v_2$$

introduces two more meaningful variables. Namely, E_C, the energy stored in the converter capacitors and D, the charge unbalance between them. Assuming that the two dc bus capacitors are equal ($C = C_1 = C_2$, $r_C = r_{C,1} = r_{C,2}$) the system dynamics using the new variables is

$$L\frac{di_f}{dt} = -r_L i_f + v_n - \alpha \tag{4}$$

$$\frac{dE_C}{dt} = -\frac{2E_C}{r_C C} + i_f \alpha \tag{5}$$

$$\frac{dD}{dt} = -\frac{1}{r_C C}D + i_f. \tag{6}$$

It is important to note that (4) and (6) are linear and decoupled with respect to state variable E_C. The partial state feedback and the change of variables will be applied as the lowest level control action on the closed-loop system.

III. CONTROL DESIGN

The controller is designed using a two level approach, as portrayed in Fig. 2: first, an inner current controller forces the sine wave shape for the network current and, second, an outer control loop yields the appropriate active power balance for
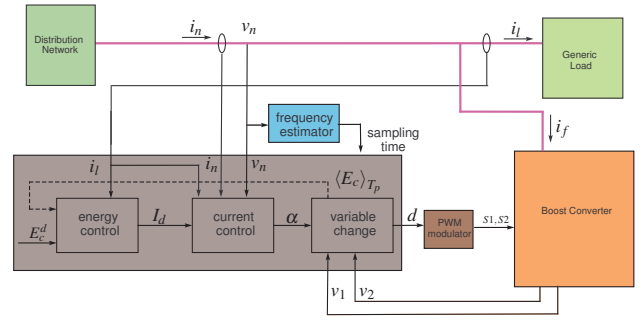
Fig. 2. Global architecture of the control system.

the whole system. The output of this loop is the amplitude of the sinusoidal reference for the current control loop. The active power balance is achieved if the energy stored in the active filter capacitors, E_C, is equal to a reference value, E_C^d.

A. The current loop controller

Taking advantage of the linearity of (4), a linear controller is designed to force a sinusoidal shape in i_n. This controller consists of two parts, as pictured in Fig. 3:

- A feedforward controller which fixes the desired steady state:

$$i_n^* = I_d^* \sin(\omega_n t) \tag{7}$$

- A feedback controller which compensates uncertainties and assures closed-loop stability.

As previously stated, the current control goal is to assure that

$$i_n^* = I_d^* \sin(\omega_n t) = i_f(t) + i_l(t),$$

where I_d^* is constant in steady state. From the circuit topology and (4),

$$\frac{di_n}{dt} = -\frac{r_L i_n}{L} - \frac{\alpha}{L} + \frac{v_n}{L} + \frac{di_l}{dt} + \frac{r_L i_l}{L}. \tag{8}$$

In order to force i_n to achieve the desired value (7), it is necessary that α takes the value

$$\alpha_{ff} = v_n + \left(L\frac{d}{dt} + r_L\right)i_l - (r_L \sin(\omega_n t) + L\omega_n \cos(\omega_n t))I_d$$

$$= v_n + F(i_l) + M(I_d, t, \omega_n), \tag{9}$$

thus defining the nominal control action that may keep the system tracking the desired trajectory. Hence, it is used as a
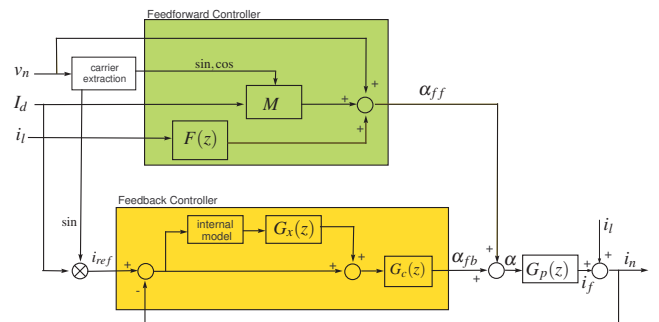
Fig. 3. Current control block diagram.

feedforward action. As the system is digitally implemented, the operator F is approximated by

$$F(z) = \frac{(L + T_s r_L) z - L}{T_s z}.$$

This action is combined with a feedback controller to overcome model uncertainties, disturbances and measurement noise.

The discrete-time model of (4), once filtered by an anti-aliasing device with time constant τ, answers to:

$$G_p(z) = \mathscr{Z} \left[\frac{-1}{Ls + r_L} \cdot \frac{1}{\tau s + 1} \cdot \frac{1 - e^{-T_s}}{s} \right]_{T_s} \quad (10)$$

As the signal to be tracked and rejected in this system is an odd-harmonic periodic one, it is convenient to design a controller which allows to track/reject this type of signal. A technique that has been proved to be specially suitable for this case is odd-harmonic repetitive control [9].

Repetitive controllers are composed of an internal model, which assures steady-state performance, and a stabilizing controller, $G_x(z)$, which assures closed-loop stability. Traditionally, repetitive controllers are implemented in a "plug-in" fashion, i.e. the repetitive compensator is used to augment an existing nominal controller, $G_c(z)$ (see Fig. 3). This nominal compensator is designed to stabilize the plant, $G_p(z)$, and provides disturbance attenuation across a broad frequency spectrum. The internal model used in odd-harmonic repetitive control [9] has the form

$$G_{im}(z) = \frac{-H(z)}{z^{\frac{N}{2}} + H(z)},$$

where $N = \frac{T_p}{T_s}$ and $H(z)$ is a low pass filter used to improve system robustness. It is important to note that N corresponds to the discrete-time period of the signal to be tracked/rejected and its value is structurally introduced in the control system. In this work the values $T_p = \frac{1}{50}$ s and $N = 400$ have been selected to obtain a good reconstruction of the continuous-time signals.

The closed-loop system of Fig. 3 is stable if the following conditions are fulfilled [9]:

1) The closed loop system without the repetitive controller is stable, i.e.

$$G_o(z) = \frac{G_c(z) G_p(z)}{1 + G_c(z) G_p(z)}$$

is stable. It is advisable to design the controller $G_c(z)$ with a high enough robustness margin. In this work, the lag controller

$$G_c(z) = -\frac{0.6305z - 0.629}{z - 0.9985}$$

provides a phase margin of 140°.

2) $\| H(z) \|_\infty < 1$. $H(z)$ is designed to have gain close to 1 in the desired bandwidth and attenuate the gain out of it. The first order linear-phase FIR filter

$$H(z) = \frac{1}{4} \cdot z + \frac{1}{2} + \frac{1}{4} \cdot z^{-1}$$

has proved to be good enough in this application.

3) $\| 1 - G_o(z) G_x(z) \|_\infty < 1$, where $G_x(z)$ is a design filter to be chosen. A trivial structure[4] which is often used is [10]:

$$G_x(z) = \frac{k_r}{G_o(z)}.$$

In this application $k_r = 0.3$ has been selected [11]. The repetitive controller defines the feedback law

$$\alpha_{fb} = G_c(z) \left[1 + G_x(z) G_{im}(z) \right] \left(i_{ref} - i_n \right)$$

that will be used with the feedforward action given in (9), this yielding $\alpha = \alpha_{fb} + \alpha_{ff}$. Fig. 3 shows the complete current control loop that will be used in the system.

Under the combined action of the feedforward and the feedback control action, one can assume that the network current is $i_n(t) \approx I_d(t) \sin(\omega_n t)$, which will be taken as a fact.

B. The energy shaping controller

Following [12], the outer controller that assures a mean value[5] of the energy stored in the capacitors, i.e. $\langle E_c(t) \rangle_{T_p}$ close to the desired reference value E_c^d, is made up of two parts (see Fig. 4):

- A feedforward term which makes $I_d^{ff} = a_0$. This assures the energy balance in the ideal case ($r_L = 0$ and $r_C = 0$) and takes into account i_l characteristics and changes instantaneously. I_d^{ff} is calculated using an amplitude modulator with a scaled signal of the source voltage as a carrier and a mean value extraction. This last operation has been implemented through the filter

$$P(z) = \frac{1}{N} \cdot \frac{1 - z^{-N}}{1 - z^{-1}},$$

which corresponds to a good approximation of the corresponding continuous-time mean value extraction operation.
- A feedback term which compensates dissipative effects and system uncertainties.

The dynamics of the plant can be modeled by the discrete-time integrator

$$\frac{T_s(z + 1)}{2(z - 1)}$$

---

[4]There is no problem with the improperness of $G_x(z)$ because the internal model provides the repetitive controller with a high positive relative degree.

[5]$\langle f(t) \rangle_{T_p} = \frac{1}{T_p} \int_{t - T_p}^{t} f(\tau) d\tau$.
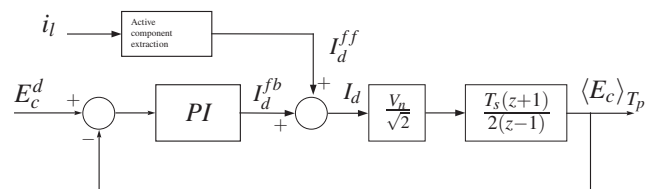
Fig. 4. Simplified 50Hz energy (voltage) control loop.
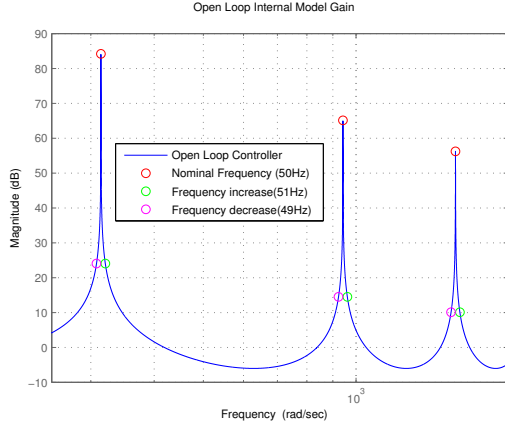
Fig. 5. Open-loop transfer function gain diagram.

and the losses in the inductor and capacitors parasitic resistances can be considered as an additive disturbance. So, the PI controller

$$I_d^{fb} = k_i \frac{T_s(z+1)}{2(z-1)}\Delta E + k_p \Delta E, \qquad (11)$$

where $\Delta E = E_c^d - \langle E_c(t) \rangle_{T_p}$, will regulate $\langle E_c(t) \rangle_{T_p}$ to the desired value E_c^d with null steady-state error.

C. Network frequency variations

Most control algorithms in the previous section contain the ratio $N = \frac{T_p}{T_s}$, i.e. the period T_p of the signals to be tracked or attenuated over the sampling period T_s. In systems where the period of the signal T_p is kept constant, N and T_s are designed a priori according to the desired number of samples per period and the technological constrains over T_s. However, in this case, the electrical distribution network frequency can undergo fluctuations and, then, T_p can not be assumed constant.

If T_p varies, the value of N or T_s should be changed in order to preserve the ratio $N = \frac{T_p}{T_s}$. If this is not the case the control algorithm performance may dramatically decay. As an example, Fig. 5 shows the feedback control open-loop gain designed for a nominal frequency of 50Hz with the gain for 49Hz, 50Hz and 51Hz (and some of their harmonics) highlighted. Note that while for the 50Hz signal the gain is important, it decays for the other frequencies. Something similar occurs with the phase lag of the closed-loop control system. While for the nominal frequency the phase is almost zero, this is not the case for the other frequencies. It is worth emphasizing that, for the active filter, this would imply a reduction of the harmonic rejection capabilities and the introduction of reactive current in the system. Clearly, both effects would contribute to the reduction of the system performance. To overcome this problem, the sample time T_s will be adaptively varied in order to maintain a constant value for N.

However, the change of T_s implies changes in the system dynamics and, particularly in the plant model, $G_p(z)$. It is important to check that these changes does not imply a

loss of closed-loop stability. Next section is devoted to this subject.

IV. STABILITY ANALYSIS

Let the discrete-time state-space representations of the blocks G_i be denoted by (A_i, B_i, C_i, D_i), $i \equiv \{im, x, c, p\}$. The closed-loop system state equations are derived under the following assumptions:

- In repetitive controllers with the structure of Figure 3 it is $D_{im} = 0$.
- The continuous-time plant $G_p(s)$ has, at least, relative degree 1, so $D_p = 0$.
- The representations corresponding to blocks $G_{im}(z)$, $G_x(z)$ and $G_c(z)$ are obtained from the nominal sampling time $T_s = \bar{T}$ and remain constant $\forall t$.
- Only the plant discrete-time model matrices A_p, B_p, vary according to sampling rate updating: $A_p = A_p(T_s)$, $B_p = B_p(T_s)$, while C_p is maintained constant. Hence, assuming that $(A, B, C, 0)$ stands for the continuous-time plant state-space representation, i.e. $G_p(s) = C(s\mathbb{I} - A)^{-1}B$, then

$$A_p(T) \triangleq e^{AT}, \quad B_p(T) \triangleq \int_0^T e^{Ar}B\,dr. \qquad (12)$$

Let the system be sampled at time instants $\{t_0, t_1, \dots\}$, with $t_0 = 0$, $t_{k+1} > t_k$, the sampling periods being $T_k = t_{k+1} - t_k$. Let also $x_k \triangleq x(t_k)$, $r_k \triangleq r(t_k)$, $y_k \triangleq y(t_k)$. The state equations are given by the discrete-time LTV system:

$$x_{k+1} = \Phi(T_k)x_k + \Pi(T_k)r_k, \quad y_k = \Upsilon x_k, \qquad (13)$$

where

$$\Phi(T) \triangleq \begin{pmatrix} K & L \\ B_p(T)M & A_p(T) + B_p(T)N \end{pmatrix}, \qquad (14)$$

$$\Pi(T) \triangleq \begin{pmatrix} B_{im} & 0 & B_c & B_p(T)C_c \end{pmatrix}^\top,$$

K, L, M, N being constant matrices available from [13].

Assume that $G_{im}(z)$, $G_x(z)$ and $G_c(z)$ are designed to provide stability for a nominal sampling time $T_s = \bar{T}$. Hence, when $T_k = \bar{T}$, $\forall k$, the overall system is stable by construction. A methodology for studying the closed-loop behavior under non-uniform sampling period is developed below.

Next result allows to reduce the stability analysis of (13) to that of its zero-input response.

Proposition 1 ([14]): Let the sampling period, T_k, take values in a compact subset $\mathcal{T} \subset \mathbb{R}^+$. Then, the uniform exponential stability of

$$x_{k+1} = \Phi(T_k)x_k \qquad (15)$$

implies the uniform Bounded Input-Bounded Output (BIBO) stability of system (13).

Proposition 2 ([14]): Let the sampling period, T_k, take values in a compact subset $\mathcal{T} \subset \mathbb{R}^+$. If there exists a matrix P such that

$$L_{T_k}(P) = \Phi(T_k)^\top P \Phi(T_k) - P < 0, \quad \text{s.t.} \quad P = P^\top > 0, \quad (16)$$

$\forall T_k \in \mathcal{T}$, then (15) is uniformly exponentially stable.

The stability analysis follows the approach proposed in [8], where the non-uniform sampling is viewed as a nominal sampling period affected by an additive disturbance. Then, the actual problem is to quantify the "amount" of disturbance due to aperiodic sampling that the system can accommodate while preserving stability.

Proposition 3: Let $T = \bar{T}$ be a fixed sampling period and define $\theta_k = T_k - \bar{T}$. Then, the matrix $\Phi(T_k)$ may be written as

$$\Phi(T_k) = \Phi(\bar{T}) + \tilde{\Delta}(\theta_k)\Psi(\bar{T}), \qquad (17)$$

where

$$\tilde{\Delta}(\theta) \triangleq \begin{pmatrix} 0 & 0 \\ 0 & \Delta(\theta) \end{pmatrix}, \quad \Delta(\theta) \triangleq \int_0^\theta e^{Ar}dr, \quad (18)$$

$$\Psi(T) \triangleq \begin{pmatrix} 0 & 0 \\ A_p(T)A & A_p(T)B \end{pmatrix} \begin{pmatrix} 0 & \mathbb{I} \\ M & N \end{pmatrix}. \quad (19)$$

Notice that, using Proposition 3, the original system (15) can take the form

$$x_{k+1} = \left[\Phi(\bar{T}) + \tilde{\Delta}(\theta_k)\Psi(\bar{T}) \right] x_k, \qquad (20)$$

which allows the following interpretation [8]: (20) can be regarded as the LTI system

$$\Sigma := \begin{cases} x_{k+1} & = & \Phi(\bar{T})x_k + u_k \\ v_k & = & \Psi(\bar{T})x_k, \end{cases} \qquad (21)$$

$G_{\bar{T}}(z) = \Psi(\bar{T})\left[z\mathbb{I} - \Phi(\bar{T})\right]^{-1}$ being its associated discrete-time transfer function, receiving the time-varying output feedback control action $u_k = \tilde{\Delta}(\theta_k)v_k$.

From now on, let $\|R\| = \left[\rho(R^\top R)\right]^{1/2}$ denote the 2-norm of a real matrix R, with $\rho(\cdot)$ standing for the spectral radius.

Theorem 4 ([8]): Assume that $T = \bar{T}$ is a nominal sampling period. Let

$$\gamma_{\bar{T}} = (1+\varepsilon)\|G_{\bar{T}}(z)\|_\infty, \quad \varepsilon > 0, \qquad (22)$$

be an upper bound of the H_∞-norm of system Σ (21), and let also $\mathscr{T} \subset \mathbb{R}^+$ be compact. If

$$\gamma_{\bar{T}}\|\Delta(T - \bar{T})\| \leq 1, \quad \forall T \in \mathscr{T}, \qquad (23)$$

then system (13) is uniformly BIBO stable in $\mathscr{T}$.

The application of the above results to the active filter is carried out straightforward. The continuous-time plant is

$$G_p(s) = -\frac{1}{2.8544 \cdot 10^{-8}s^2 + 0.000081784s + 0.5}, \quad (24)$$

where $L = 0.8mH$, $r_L = 0.5\Omega$ and $\tau = 3.568 \cdot 10^{-5}s$. The controller is constructed for a nominal frequency of $\bar{v} = 50$ Hz, and $N = 400$ is selected to obtain a good reconstruction of the continuous-time signals; this yields a nominal sampling period of $\bar{T} = \bar{T}_p N^{-1} = (N\bar{v})^{-1} = 0.05$ ms. Notice that the closed-loop system order is high, because the dimensions of Φ are now 209×209. Under these assumptions, (10) becomes

$$G_p(z) = -\frac{0.02855z + 0.01783}{z^2 - 1.215z + 0.2387}. \qquad (25)$$

These settings yield $\|G_{\bar{T}}(z)\|_\infty = 2.6530 \times 10^4$. In order to define $\gamma_{\bar{T}}$ (see (22)), $\varepsilon = 0.0001$ has been selected. Recall
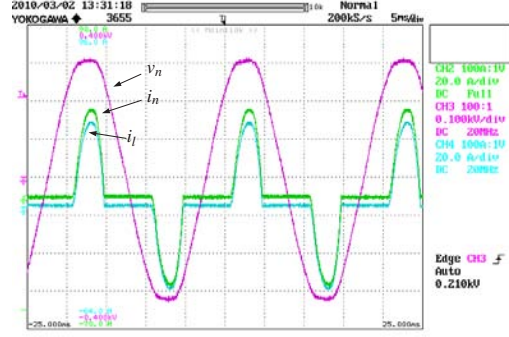
Fig. 6. Nonlinear load connected to the grid (50Hz): v_n, i_n and i_l vs time (The active filter is off).

now that the continuous-time plant matrix can be obtained from (24). Then, according to Theorem 4, the stability interval for the network frequency obtained from a numeric computation of norm bounds for the matrix exponential Δ (see (23)) is [42.4676, 59.3855] Hz. It is worth mentioning that line frequency variations use to be, at most, a 10% of its nominal value, i.e. they can be expected to lie inside the interval [45, 55] *Hz*.

V. EXPERIMENTAL SETUP AND RESULTS

A. Experimental setup

The experimental setup is composed of a full-bridge diode rectifier (nonlinear load), the previously described single-phase active filter, the regular distribution network and ac power source (*PACIFIC Smartsource, 140-AMX-UPC12*) that acts as a variable frequency ac source[6]. The active filter is connected in a shunt manner with the rectifier to compensate its distorted current.

The active filter controller has been implemented on a DSP based hardware, i.e. within a digital framework, with a nominal sampling frequency equal to the switching frequency of 20 kHz. The network frequency is obtained from the network voltage zero crossings through some additional hardware and a digital lowpass filter that runs in the DSP. With this information, the sampling frequency is updated to maintain the ratio $N = 400$.

B. Experimental results

Fig. 6 shows the waveforms of v_n, i_l and i_n when the nonlinear load is connected to the network. The rectifier current has a total harmonic distortion(THD) of 62.6% and RMS value of 19.56A.

As Fig. 7 shows, when the active filter is connected in parallel with the rectifier the shape of the current at the source port is nearly sinusoidal with a THD of 1.2% while the power factor (PF) and $\cos\phi$ at the port are unitary. The figure shows that the mean value of v_1 is maintained almost constant[7].

In the next experiment the network frequency of the system changes from 48Hz to 53Hz in a 20 cycles ramp

---

[6]Used only in the varying frequency experiments or when not working at the nominal frequency.

[7]v_2 is not show due the limited number of channels in the instrumentation.
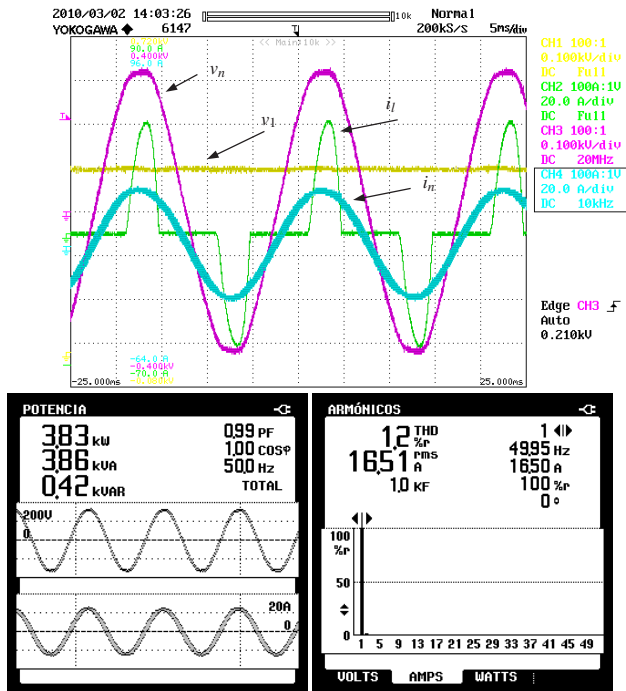
Fig. 7. Nonlinear load and the active filter connected to grid network (50Hz). (top) v_n, i_n, i_l and v_1 *vs* time; (bottom) PF, $\cos\phi$ and THD for i_n.

Fig. 8. Nonlinear load and the active filter: (top) v_n, i_n, i_l and v_1 *vs* time when the network frequency changes from 48Hz to 53Hz in a 20 cycles ramp manner; (bottom) v_n, i_n, PF, $\cos\phi$ and THD for i_n when the system reaches the steady state at 52 Hz.

manner (in this experiment the ac power source is used to feed the nonlinear load). The response of v_n, i_n, i_l and the semibus voltage v_1 is plotted in Fig. 8 (top). As it can be seen, all variables are bounded and the mean value of v_1 is almost constant.

Additionally, Fig. 8 depicts the system behavior in the steady state at 52Hz. As it can be shown the PF and the $\cos\phi$ return to unitary values and the THD for i_n is 0.4% (in this experiment the ac power source is used to feed the nonlinear load).

VI. CONCLUSIONS

This work shows the architecture, some design issues and a stability analysis for an active filter digital controller based on repetitive control. The controller includes a mechanism to follow possible network frequency variations without losing the advantages of the repetitive control and maintaining its low computational cost. In turn, the stability analysis is based on the small-gain theorem. Theoretical and experimental results prove that the controlled system has a good performance and that, using the frequency adaptation mechanism, it is able to cope with more aggressive frequency changes than the usual ones in electrical distribution networks.

REFERENCES

[1] S. Buso, L. Malesani, and P. Mattavelli, "Comparison of current control techniques for active filters applications," *IEEE Trans. on Industrial Electronics*, vol. 45, pp. 722–729, october 1998.
[2] P. Mattavelli, "A closed-loop selective harmonic compensation for active filters," *IEEE Trans. on Industry Applications*, vol. 37, no. 1, pp. 81–89, january 2001.
[3] R. Costa-Castelló, R. Griñó, R. Cardoner Parpal, and E. Fossas, "High-performance control of a single-phase shunt active filter," *IEEE Transactions on Control Systems Technology*, vol. 17, no. 6, pp. 1318–1329, Nov. 2009.
[4] T. J. Manayathara, T. Tsao, and J. Bentsman, "Rejection of unknown periodic load disturbances in continous steel casting process using learning repetitive control approach," *IEEE Transactions on Control Systems Technology*, vol. 4, no. 3, pp. 259–265, May 1996.
[5] J. Liu and Y. Yang, "Frequency adaptive control technique for rejecting periodic runout," *Control Engineering Practice*, vol. 12, pp. 31–40, 2004.
[6] R. Costa-Castelló, S. Malo, and R. Griñó, "High performance repetitive control of an active filter under varying network frequency," in *IFAC WORLD CONGRESS 2008*, Seoul. Korea, Jul.6-11, 2008, pp. 1–6.
[7] G. A. Ramos, J. M. Olm, and R. Costa-Castelló, "Digital repetitive control under time-varying sampling period: An lmi stability analysis," in *Proc. IEEE Control Applications, (CCA). Intelligent Control, (ISIC)*, Saint Petersburg, Russia, Jul. 8–10, 2009, pp. 782–787.
[8] H. Fujioka, "Stability analysis for a class of networked-embedded control systems: A discrete-time approach," in *Proceedings of the 2008 American Control Conference*, pp. 4997–5002.
[9] R. Griñó and R. Costa-Castelló, "Digital repetitive plug-in controller for odd-harmonic periodic references and disturbances," *Automatica*, vol. 19, no. 4, pp. 1060– 1068, July 2004.
[10] M. Tomizuka, T. Tsao, and K. Chew, "Analysis and synthesis of discrete-time repetitive controllers," *Journal of Dynamic Systems, Measurement, and Control*, vol. 111, pp. 353–358, September 1989.
[11] G. Hillerström and R. C. Lee, "Trade-offs in repetitive control," University of Cambridge, Tech. Rep. CUED/F-INFENG/TR 294, June 1997.
[12] R. Costa-Castelló, R. Griñó, R. Cardoner, and E. Fossas, "High performance control of a single-phase shunt active filter," in *Proc. of the 2007 IEEE International Symposium on Industrial Electronics (ISIE 2007)*, june 2007, pp. 3350–3355.
[13] G. Ramos, J. Olm, and R. Costa-Castelló, "Non-uniform sampling in digital repetitive control systems: an LMI stability analysis," *Technical Report n. IOC-DT-P-2009-01, Universitat Politècnica de Catalunya*, 2009, available online at: http://hdl.handle.net/2117/2651.
[14] W. Rugh, *Linear system theory, 2nd Ed.* Prentice-Hall, Inc., Upper Saddle River, NJ, 1996.